HHS Public Access

Author manuscript

Mol Microbiol. Author manuscript; available in PMC 2017 June 01.

Published in final edited form as:

Mol Microbiol. 2016 June ; 100(6): 954–971. doi:10.1111/mmi.13361.

A Novel Regulator Controls *Clostridium difficile* Sporulation, Motility and Toxin Production

Adrianne N. Edwards[1], **Rita Tamayo**[2], and **Shonna M. McBride**[1,*]

[1]Department of Microbiology and Immunology, Emory University School of Medicine, Atlanta, GA, USA

[2]Department of Microbiology and Immunology, University of North Carolina at Chapel Hill, Chapel Hill, NC, USA

SUMMARY

Clostridium difficile, is an anaerobic pathogen that forms spores which promote survival in the environment and transmission to new hosts. The regulatory pathways by which *C. difficile* initiates spore formation are poorly understood. We identified two factors with limited similarity to the Rap sporulation proteins of other spore-forming bacteria. In this study, we show that disruption of the gene *CD3668* reduces sporulation and increases toxin production and motility. This mutant was more virulent and exhibited increased toxin gene expression in the hamster model of infection. Based on these phenotypes, we have renamed this locus *rstA,* for regulator of sporulation and toxins. Our data demonstrate that RstA is a bifunctional protein that upregulates sporulation through an unidentified pathway and represses motility and toxin production by influencing *sigD* transcription. Conserved RstA orthologs are present in other pathogenic and industrial *Clostridium* species and may represent a key regulatory protein controlling clostridial sporulation.

Keywords

Clostridium difficile; sporulation; spore; anaerobe; tetratricopeptide repeat domains; toxin production; motility; Spo0A; SigD; TcdA; TcdB; RNPP; RRNPP

INTRODUCTION

For the obligate anaerobe *Clostridium difficile*, the formation of a dormant spore is a critical transition within its life cycle. *C. difficile* spore formation permits long-term persistence outside the host, provides recalcitrance from anti-infectives and facilitates efficient transmission from host to host (Deakin *et al.*, 2012). While *C. difficile* exhibits the same morphological features throughout each sporulation stage as the model organism, *B. subtilis*, many of the regulatory proteins that control the early stages of sporulation are not conserved or readily apparent within the *C. difficile* genome (Paredes *et al.*, 2005, Pereira *et al.*, 2013,

*Corresponding author. Mailing address: Department of Microbiology and Immunology, Emory University School of Medicine, 1510 Clifton Rd, Atlanta, GA 30322. Phone: (404) 727-6192. Fax: (404) 727-8250. shonna.mcbride@emory.edu.

The authors declare no competing financial interests.

Saujet *et al.*, 2013, Fimlaid *et al.*, 2013, Edwards & McBride, 2014). Therefore, the regulatory mechanisms that govern the initiation of spore formation in *C. difficile* are mostly unknown, with only a few regulatory proteins identified and studied thus far (Underwood *et al.*, 2009, Saujet *et al.*, 2011, Deakin *et al.*, 2012, Edwards *et al.*, 2014, McBride, 2014). These include the master regulator of sporulation, Spo0A, which is a highly conserved transcriptional regulator, and the stationary phase sigma factor, SigH, both of which are found in all studied endospore-formers. Spo0A and SigH regulate the expression of early sporulation-specific genes and are required for the initiation of sporulation (Deakin *et al.*, 2012, Rosenbusch *et al.*, 2012, Saujet *et al.*, 2011).

Recently, our work revealed that *C. difficile* initiates sporulation in response to nutrient availability and uptake (Edwards *et al.*, 2014). The loss of two oligopeptide permeases, Opp and App, results in increased sporulation, likely due to the inability of the mutant to import small peptides as a nutrient source (Edwards *et al.*, 2014). In other Gram-positive species, Opp and App also import small quorum sensing peptides, which control a vast array of physiological processes, including sporulation, competence, conjugation, toxin expression and production of other virulence factors (Rudner *et al.*, 1991, Perego *et al.*, 1991, Koide & Hoch, 1994, Leonard *et al.*, 1996, Solomon *et al.*, 1996, Gominet *et al.*, 2001, Chang *et al.*, 2011). In *B. subtilis*, the Phr quorum sensing peptides positively regulate sporulation initiation. The Phr peptides are synthesized within the cell, exported and processed, accumulate in high cell density conditions, and are then imported back into the cell by Opp and App (Perego & Hoch, 1996, Perego, 1997, Jiang *et al.*, 2000). Once inside the cell, the Phr peptides promote sporulation by binding to and inhibiting the activity of the Rap phosphatases (Perego, 1997, Lazazzera *et al.*, 1997). The Rap phosphatases indirectly prevent phosphorylation of Spo0A and thus, inhibit spore formation (Perego *et al.*, 1994). This regulatory pathway is one of several in *B. subtilis* that modulate the level of phosphorylated (active) Spo0A, thereby ensuring that sporulation initiation is appropriately controlled.

The *B. subtilis* Rap phosphatases belong to the RNPP (Rap/NprR/PlcR/PrgX) family of cytoplasmic proteins (Declerck *et al.*, 2007), or the RRNPP family, to include the *Streptococcus* Rgg proteins (Mashburn-Warren *et al.*, 2010, Parashar *et al.*, 2015). The *C. difficile* genome encodes two potential RNPP proteins (CD2123 and CD3668) (Edwards & McBride, 2014, Edwards *et al.*, 2014). This study was undertaken to determine whether either RNPP-like protein has a role in *C. difficile* spore formation. Herein, we describe one RNPP ortholog, CD3668, which regulates multiple physiological traits *in vitro*, including sporulation, motility and toxin production. Our results also indicate that CD3668 is a bifunctional protein that influences spore formation and toxin expression *in vivo* and is important for virulence in an animal model of CDI. This study provides the first evidence that an RNPP protein controls spore formation and other virulence traits in *Clostridium* and closely related organisms.

RESULTS

Identification and disruption of two putative RNPP orthologs in *C. difficile*

CD2123 and CD3668 possess multiple, conserved tetratricopeptide repeat (TPR) domains, which are a core feature of Gram-positive proteins belonging to the RNPP (Rgg/Rap/NprR/PlcR/PrgX; or RRNPP) family (Declerck *et al.*, 2007, Parashar *et al.*, 2015; Fig. 1). The Rap proteins directly bind and dephosphorylate their molecular target: Spo0F, a member of the phosphorylation-dependent pathway that activates Spo0A, and ComA, the regulator of competence in *Bacillus* species (Perego *et al.*, 1994, Core & Perego, 2003, Bongiorni *et al.*, 2005). The other RNPP members include the *Bacillus* NprR and PlcR, the *Enterococcus* PrgX and *Streptococcus* Rgg proteins, which are DNA-binding transcription factors. NprR from *Bacillus thurigiensis* contains a bifunctional N-terminal region comprised of a helix-turn-helix (HTH) DNA-binding domain followed by a Spo0F-binding domain (Cabrera *et al.*, 2014). NprR is the only published dual-function protein in the RNPP family.

Neither CD2123 nor CD3668 encode an identifiable phosphatase domain, a hallmark feature of the Rap phosphatase proteins. Besides the TPR domains identified within CD2123, this protein does not encode any other apparent protein motifs. The CD3668 sequence contains a conserved HTH DNA-binding motif in the N-terminal region, followed by five TPR repeat regions (Fig. 1). Protein structure modeling analysis using Phyre2 (Kelley *et al.*, 2015) revealed that the predicted structure of CD3668 models to several members of the RNPP family, including PlcR of *Bacillus thuringiensis*, NprR of the *Bacillus cereus* group and RapH, RapI and RapJ from *B. subtilis*. There is a high degree of similarity in CD3668 to both the N-terminal HTH DNA-binding motif and the peptide-interacting TPR domains of PlcR and NprR (Grenha *et al.*, 2013). Although there is structural similarity between CD3668 and the *B. subtilis* RapH, RapI and RapJ proteins, only 4 of 18 identified amino acids required for Rap-dependent Spo0F-binding and dephosphorylation are conserved in CD3668 (Parashar *et al.*, 2011, Parashar *et al.*, 2013; not shown). Altogether, these structural analyses provide evidence that CD3668 is related to the transcriptional regulators in the RNPP family. While the predicted Phyre2-generated protein structure of CD2123 is predominantly alpha-helical, there was little similarity to any prokaryotic proteins, suggesting that CD2123 may function differently than other RNPP proteins.

Disruption of *CD3668* decreases sporulation frequency in *C. difficile*

In *Bacillus* species, the Rap and NprR proteins inhibit sporulation by directly binding and dephosphorylating Spo0F, an intermediate phosphotransfer protein in the sporulation phosphorelay (Perego *et al.*, 1994, Cabrera *et al.*, 2014). The sporulation phosphorelay modulates the phosphorylation state of the master sporulation regulator, Spo0A, in response to a variety of intracellular and environmental signals. Many of the *B. subtilis* Rap proteins inhibit sporulation; hence, overexpression of these proteins lowers the sporulation frequency while null mutations in these loci often result in increased sporulation frequency (Perego *et al.*, 1994, Mueller & Sonenshein, 1992). There is no sporulation phosphorelay encoded in the *C. difficile* genome (Paredes *et al.*, 2005, Sebaihia *et al.*, 2006). In *C. difficile,* Spo0A appears to be activated by phosphorylation directly by sporulation kinases (Underwood *et*

al., 2009), and it is expected that Spo0A can be directly inactivated, as well (Paredes *et al.*, 2005, Edwards & McBride, 2014, Underwood *et al.*, 2009).

To determine if CD2123 or CD3668 is important for *C. difficile* spore formation, we created independent insertional mutations in these genes. Antibiotic resistance markers were introduced in *CD2123* at nucleotide 553 and in *CD3668* at nucleotide 306, using a TargeTron-based group II intron. The presence of the retargeted intron in the correct gene was confirmed by Southern blot analysis (Fig. S1A), and qRT-PCR analysis confirmed a significant reduction of *CD2123* and *CD3668* transcript levels in the respective mutants (Fig. S1B and S1C). Transcription of *CD3667, CD3666 and CD3665*, the genes immediately downstream of *CD3668*, were slightly decreased in the *CD3668* mutant (Fig. S1C), while *CD3664* expression was unchanged. PCR analysis of cDNA from 630Δ*erm* confirmed that *CD3668-CD3667-CD3666-CD3665-CD3664* constitute a transcriptional unit (Fig. S1D, E); however, our transcriptional data suggest that the full 3.83 kb region may be a minor product since transcript levels of the downstream genes are not as greatly affected by the insertional mutation in *CD3668. CD3667* is annotated as a selenium metabolism protein, *CD3666* and *CD3665* as hypothetical proteins and *CD3664* as an aminotransferase, and are all uncharacterized, to our knowledge.

The *CD2123* and *CD3668* mutants (MC379 and MC391, respectively) were tested for sporulation frequency after 24 h of growth (H_{24}) on 70:30 sporulation agar (Putnam *et al.*, 2013). Using phase-contrast microscopy to differentiate vegetative bacilli from phase bright spores, we observed a mean sporulation frequency of 28.1% in the parent strain, 630Δ*erm* (Fig. 2A), consistent with previously published results (Putnam *et al.*, 2013). The *CD2123* mutant demonstrated a similar sporulation frequency to the parent strain (Fig. 2A). In contrast, the *CD3668* mutant produced ~20-fold less spores than the parent strain (1.4% in the *CD3668* versus 28.1% in 630Δ*erm*; Fig. 2A), suggesting that CD3668 is important for sporulation in *C. difficile*. When enumerating ethanol resistant spores from strains grown on 70:30 sporulation agar at H_{24}, a ~25-fold decrease in sporulation frequency in the *CD3668* mutant compared to 630Δ*erm* was observed (Table 1), which corroborates the oligosporogenous phenotype ascertained with phase contrast microscopy. When a plasmid copy of *CD3668*, driven by the nisin-inducible *cprA* promoter (McBride & Sonenshein, 2011b, McKee *et al.*, 2013), was introduced into the *CD3668* mutant (MC480), the sporulation phenotype was partially restored in a manner relative to the amount of inducer added to the medium (Fig. 2B). The sporulation frequency of the *CD3668* mutant containing the pP*cprA-CD3668* construct (MC480) was 1.9% in the absence of nisin, and increased to 13.3% in 0.5 μg ml^{-1} nisin and 17.3% in 1 μg ml^{-1} nisin (Fig. 2B), confirming that CD3668 positively influences sporulation in *C. difficile*. The inability to fully complement the sporulation phenotype may be due to exogenous *CD3668* expression driven from an inducible promoter on a plasmid, rather than from the native promoter on the chromosome, which may not reflect native expression patterns. Overexpression of *CD3668* in the parent background (MC478) did not increase sporulation frequency (Fig. 2B).

Sporulation is a complex process in bacteria and is defined by multiple morphological stages (Errington, 2003, Pereira *et al.*, 2013, Paredes-Sabja *et al.*, 2014). Specific genetic and regulatory events are required to complete each morphological stage throughout sporulation

(Losick & Stragier, 1992, Fimlaid *et al.*, 2013, Saujet *et al.*, 2013, Pereira *et al.*, 2013). To further assess the sporulation phenotype of the *CD3668* mutant, we performed fluorescence microscopy using the membrane specific dyes, FM4-64 and Mitotracker green (MTG). This technique allows the detection of earlier sporulation events, such as asymmetric septum formation (stage II) and engulfment of the prespore (stage III), neither of which is visible by phase contrast microscopy. At H_{24}, there was a significant decrease in cells at stage II or beyond in the *CD3668* mutant (6.1 ± 1.7%) compared to the parent strain (35.2 ± 3.9%; Fig. 2C), indicating that fewer cells are able to achieve mature spore formation in the *CD3668* mutant compared to the parent strain. As there is no increase in sporulation frequency in the *CD3668* mutant at H_{96} compared to H_{24} (Fig. S2), it is likely that sporulation in the *CD3668* mutant is arrested early.

Sporulation-specific gene expression is decreased in the *CD3668* mutant

The decreases in sporulation frequency and in the formation of asymmetric sporulation septa in the *CD3668* mutant suggest that sporulation-specific gene expression is reduced and/or delayed in this strain. To further characterize the sporulation phenotype of the *CD3668* mutant, we used qRT-PCR to measure the transcript levels of *spo0A* and the sporulation-specific sigma factors at multiple time points during growth on 70:30 sporulation agar. Transcription of *spo0A*, which encodes the master regulator of sporulation, was unchanged between the parent strain and the *CD3668* mutant (Fig. 3A). However, *spo0A* transcript levels do not fully correlate to Spo0A~P activity (Edwards *et al.*, 2014), as is frequently observed with regulatory proteins. To evaluate Spo0A~P activity, we also analyzed transcription of *sigE*, an early stage sporulation-specific sigma factor that depends upon active Spo0A~P for its expression. We found that *sigE* expression appeared decreased at H_8 and H_{10} and was significantly decreased at H_{12} in the *CD3668* mutant (~6-fold; Fig. 3B). Transcript levels of additional sporulation-specific sigma factors, *sigF* and *sigG*, trended lower at H_8 and H_{10} and were significantly decreased at H_{12} in the *CD3668* mutant (~2-fold and ~7-fold, respectively; Fig. 3C–D). Further, expression of another Spo0A-dependent gene, *spoIIE*, which encodes a phosphatase necessary for SigF activation, was also significantly decreased in the *CD3668* mutant (Fig. S3A). These data indicate that sporulation-specific genes are expressed at lower levels in the *CD3668* mutant, which correlates with the reduced sporulation phenotype observed.

As Spo0A activity is controlled by phosphorylation, we analyzed the expression of the three putative Spo0A sensor histidine kinases in *C. difficile* (Underwood *et al.*, 2009). Transcript levels of *CD1492*, *CD1579* and *CD2492* were all increased in the absence of *CD3668* (Fig. S3B), which suggests that levels of phosphorylated Spo0A would be higher in the *CD3668* mutant, contradicting the pattern of sporulation-specific gene expression observed above. Because the function of these three putative Spo0A kinases are not elucidated, there are likely additional regulatory interactions unknown that control sporulation initiation. Finally, *sigE* transcript levels were similarly decreased (~4-fold) in the *CD3668* mutant grown in TY medium compared to growth on 70:30 sporulation agar (Fig. S4A versus Fig. 4B), indicating that CD3668 controls sporulation in multiple growth conditions.

Toxin gene expression and toxin production are increased in the *CD3668* mutant

Sporulation and the production of the two primary *C. difficile* toxins, toxin A (TcdA) and toxin B (TcdB), have been linked in multiple *C. difficile* strains (Deakin *et al.*, 2012, Mackin *et al.*, 2013, Pettit *et al.*, 2014), although a definitive regulatory pathway has not been identified. To determine whether the loss of *CD3668* affects toxin production, we first analyzed *tcdA* and *tcdB* gene expression using qRT-PCR. Transcript levels of *tcdA* and *tcdB* were elevated in the *CD3668* mutant when grown on 70:30 sporulation agar (~4-fold and ~3.5-fold, respectively; Fig. 4A) or in TY medium (~6-fold; Fig. S4A), suggesting that CD3668 negatively influences toxin gene expression. Both *tcdA* and *tcdB* gene expression were complemented to wild-type levels when *CD3668* expression was induced in the *CD3668* mutant (Fig. S5A, B). Additionally, *CD3668* overexpression in the 630Δ*erm* parent background resulted in a ~2-fold decrease in *tcdA* transcript levels (Fig. S5A), further confirming that CD3668 represses toxin gene expression. Western blot analysis of cultures grown in TY medium demonstrated that TcdA protein levels were increased ~2.1-fold in the *CD3668* mutant compared to the 630Δ*erm* parent (Fig. 4B). No change in TcdA protein levels was detected in the *CD2123* mutant (Fig. 4B), analogous to the toxin expression profiles for this strain (Fig. 4A).

Regulation of *C. difficile* toxin production is complex and is influenced by multiple regulatory factors. Expression of *tcdA* and *tcdB* is directly activated by the toxin-specific sigma factor, TcdR (Mani & Dupuy, 2001), while the motility sigma factor, SigD, directs *tcdR* transcription (McKee *et al.*, 2013, El Meouche *et al.*, 2013; Fig. 4). In addition, toxin gene expression is directly repressed by the global regulators, CodY (Dineen *et al.*, 2007) and CcpA (Antunes *et al.*, 2011, Antunes *et al.*, 2012), in response to nutrient availability (Karlsson *et al.*, 2008). To elucidate whether CD3668 controls *tcdA* and *tcdB* transcription directly or through one of the known regulators, we assessed *tcdR* transcript levels in the *CD3668* mutant. Transcription of *tcdR* was ~3-fold higher in the *CD3668* mutant compared to the parent strain or the *CD2123* mutant (Fig. 4A). Altogether, these data indicate that CD3668 negatively affects *C. difficile* toxin production, likely through the toxin-specific sigma factor, TcdR.

CD3668 controls motility and toxin production through regulation of *sigD* expression

SigD is the only known positive regulator of the toxin-specific sigma factor, *tcdR* (El Meouche *et al.*, 2013, McKee *et al.*, 2013). As such, we next investigated the effects of *CD3668* disruption on *sigD* expression. The abundance of the *sigD* transcript was ~2.5-fold higher in the *CD3668* mutant compared to the parent strain grown on 70:30 sporulation agar (Fig. 5A), while a ~2-fold increase in *sigD* transcript occurred when grown in TY medium (Fig. S4A). The *CD2123* mutant exhibited no change in *sigD* transcript levels, while the *sigD* transcript was ~2-fold lower in the *sigD* mutant (Fig. 5A), as previously shown (El Meouche *et al.*, 2013). However, SigD is subject to post-translational regulation (El Meouche *et al.*, 2013); thus, transcript abundance of *sigD* is not fully indicative of its activity. To determine if SigD-dependent gene expression was also affected in the *CD3668* mutant, we analyzed transcript levels of *fliC*, a SigD-dependent flagellar gene. Expression of *fliC* was significantly higher in the *CD3668* mutant on 70:30 sporulation agar (Fig. 5A) and in TY medium (Fig. S4A). Likewise, *fliC* expression was significantly reduced when

CD3668 expression was induced in the *CD3668* mutant (Fig. S5C). Expression of additional SigD-regulated genes, such as the early stage flagellar genes, *flgB*, *motA* and *fliQ*, were also higher in the *CD3668* mutant (Fig. S6A), demonstrating that SigD-dependent gene expression is globally affected by the loss of CD3668. Finally, to determine if the CD3668-dependent regulation of *sigD* transcription influences motility of *C. difficile*, swimming motility assays were performed using soft agar plates. As shown in Fig. 5B, the *CD3668* mutant exhibited a ~10% increase in swimming motility at 120 h compared to the parent strain. As anticipated, the *sigD* mutant control was nonmotile.

Although the data indicate that CD3668 signals through *sigD* expression to regulate toxin production, we assessed whether CD3668 could also influence the other known regulators of toxin expression, CodY and CcpA. Transcription of *ccpA* was unaffected, and a small decrease in *codY* expression was observed in the *CD3668* mutant, but no consistent change in expression was found for genes controlled by these regulators (Fig. S6B, data not shown). Together, these results demonstrate that CD3668 regulates toxin expression in a SigD-dependent manner. Because of the phenotypes affected by CD3668, we propose this locus be renamed *rstA* (regulator of sporulation and toxin, A).

Expression of *rstA* may be controlled through autoregulation

RNPP proteins often control their own expression (Lereclus *et al.*, 1996, Lazazzera *et al.*, 1999, Mashburn-Warren *et al.*, 2010). We asked whether the *rstA* mutation affects *rstA* expression. *rstA* transcript levels slightly increased in the parent strain during growth on 70:30 sporulation agar (at H_8 and H_{12}; Fig. 6A) and remained unchanged during growth in TY medium (Fig. S4B). Expression of *rstA* was increased ~4–6-fold in the *rstA* mutant compared to the parent strain at all time points when grown on 70:30 sporulation agar (Fig. 6A) and in TY medium (~3–5-fold; Fig. S4B), which suggests that RstA negatively influences its own expression. To further assess whether RstA affects *rstA* transcription, we constructed a P*rstA::phoZ* reporter fusion containing 489 bp upstream of the annotated *rstA* start codon and measured alkaline phosphatase (AP) activity in 630Δ*erm* and the *rstA* mutant. AP activity was increased ~1.7-fold in the *rstA* mutant compared to the parent strain (Fig. 6B), further verifying that *rstA* inhibits its own expression. Altogether, these data strongly suggest that *rstA* transcription is autoregulatory.

As RNPP proteins and their cognate quorum sensing peptide are often co-transcribed or located adjacent to one another (Rocha-Estrada *et al.*, 2010, Cook & Federle, 2014), we looked for potential open reading frames that may encode a precursor to a quorum sensing peptide or a similar regulatory feature; however, no candidate, short open reading frame that possibly encodes a peptide is apparent near the *rstA* locus. It is possible, however, that the one or both of the hypothetical genes downstream of *rstA*, *CD3666* and *CD3665*, encode an unknown class of quorum sensing peptides.

The *rstA* mutant exhibits increased virulence in the hamster model of *C. difficile* infection

The TcdA and TcdB toxins are critical virulence factors in animal models of *C. difficile* infection (Kuehne *et al.*, 2010). Because RstA inhibits toxin gene expression, we next asked whether the *rstA* mutant is more virulent in a hamster model of *C. difficile* infection (Chang

et al., 1978, Douce & Goulding, 2010, Best *et al.*, 2012). Female Syrian golden hamsters were infected with the 630Δ*erm* parent strain or the *rstA* mutant. Animals were monitored for symptoms of *C. difficile* infection, as described in the Experimental Procedures. Hamsters infected with the *rstA* mutant succumbed to *C. difficile* infection more quickly than those infected with the 630Δ*erm* parent strain ($P < 0.01$, log rank test; mean times to morbidity: 45.5 ± 3.5 h for 630Δ*erm* and 34.1 ± 2.6 h for the *rstA* mutant; one animal infected with 630Δ*erm* survived the duration of the ten day study; Fig. 7A). These results indicate that the *rstA* mutant is more virulent than the parental strain.

To quantify the burden of total *C. difficile* vegetative cells and spores *in vivo*, fecal samples were collected 24 h post-infection and cecal contents were acquired at the time of morbidity. While there was no statistically significant difference in the number of *C. difficile* colony forming units (CFU) in feces 24 h post infection (Fig. 7B), significantly fewer CFU (~2.5-fold) were enumerated from cecal contents for hamsters infected with the *rstA* mutant compared to those infected with 630Δ*erm* (Fig. 7C). It is important to note that no significant *in vitro* growth defect was observed in the *rstA* mutant when grown in BHIS, TY or 70:30 sporulation media (data not shown), which may suggest that the *rstA* mutant forms fewer spores *in vivo*.

To determine if toxin gene expression was greater *in vivo*, as it is *in vitro*, RNA was isolated from the cecal contents of infected hamsters post-mortem. Cecal contents from an uninfected animal were included as a control. Expression analyses revealed that both *tcdA* and *tcdB* transcript levels were higher (~2.5- and ~1.6-fold, respectively) in animals infected with the *rstA* mutant, compared to those infected with the parent strain (Fig. 7D). Because RstA appears to control toxin expression through SigD, we also measured *in vivo sigD* transcription. Transcript levels of *sigD* were significantly higher (~2.6-fold) in hamsters infected with the *rstA* mutant (Fig. 7D), suggesting that RstA also regulates toxin production and motility in a SigD-dependent manner *in vivo*. Finally, because animals infected with the *rstA* mutant carried fewer total *C. difficile* cells *in vivo*, at the time of death (Fig. 7C), we asked whether a reduced sporulation frequency *in vivo* contributed to this phenotype. *sigE* transcription was examined in cecal contents to determine if sporulation-specific gene expression was decreased *in vivo*, as observed *in vitro*. *sigE* transcription was detected in most hamsters infected with the 630Δ*erm* strain (n = 10/11); however, *sigE* transcripts were only detectable in two of the nine hamsters tested that were infected with the *rstA* mutant, even though other transcripts were readily measurable. The inability to detect *sigE* transcript levels in most of the *rstA*-infected hamsters may correlate with the reduced number of total *C. difficile* cells recovered from cecal contents if the *rstA* mutant is oligosporogenous *in vivo.* The gene expression patterns observed in infected hamsters suggest that the same RstA-mediated regulation of sporulation and toxin production identified *in vitro,* are also relevant *in vivo*.

RstA demonstrates bifunctional control of sporulation and SigD-dependent activity

The presence of a putative HTH DNA-binding motif and protein-interacting TPR domains suggests that RstA may interact with peptides and also serve as a DNA-binding transcriptional regulator. To assess the importance of the DNA-binding domain in RstA

function, a truncated RstA lacking 37 amino acids within the HTH domain, was expressed in the *rstA* mutant and evaluated for effects on sporulation and SigD-dependent gene expression (MC738, Table 2; Cabrera *et al.*, 2014). Expression of the *rstAΔHTH* allele substantially restored sporulation of an *rstA* mutant but did not significantly affect SigD repression, as evidenced by SigD-dependent gene expression (Table 2). These results demonstrate that the HTH DNA-binding domain is dispensable for RstA-dependent stimulation of sporulation but is important for repression of SigD. Conversely, the five predicted peptide-interacting TPR domains that comprise the majority of RstA are sufficient to partially restore the sporulation-promoting functions of the protein, but are not adequate for repression of *sigD* expression.

DISCUSSION

Although *C. difficile* efficiently forms spores, many conserved regulatory proteins that are required for initiating sporulation in other studied spore-formers are not encoded in the *C. difficile* genome, suggesting that *C. difficile* employs unique regulatory mechanisms to control the early stages of sporulation. *C. difficile* does encode two weak orthologs to the Rap family of proteins, which inhibit sporulation in *Bacillus* species by indirectly preventing the accumulation of phosphorylated Spo0A, the active form of the master regulator of sporulation. In contrast, our study demonstrates that one *C. difficile* Rap-like protein, RstA (CD3668), functions as a novel regulator to increase sporulation and decrease motility and toxin production (Fig. 8).

Our results reveal that RstA regulates several physiological processes and virulence in *C. difficile* in multiple *in vitro* conditions. RstA positively affects the initiation of sporulation through its peptide-interacting TPR domains. RstA likely influences early sporulation events, as the majority of *rstA* mutant cells do not advance beyond Stage II of sporulation and gene expression of Spo0A-dependent genes and early-sporulation sigma factors is decreased. In addition, RstA negatively influences TcdA and TcdB toxin production and motility by repressing transcription of *sigD,* resulting in higher expression of toxins *in vivo* and increased virulence when the *rstA* mutant is used in the hamster model of *C. difficile* infection. Our data demonstrate that RstA regulates toxin expression through SigD, the flagellar-specific sigma factor. Removal of the HTH DNA-binding motif and examination of sporulation in a *sigD* mutant revealed that RstA controls sporulation initiation through a SigD-independent pathway. Based on these results, we hypothesize that RstA may be a global regulator in *C. difficile*, similar to the broad physiological roles RNPP proteins play in other bacteria.

While RstA exhibits more amino acid similarity to the *Bacillus* Rap proteins, RstA shares more features in common with the other members of the RNPP family of proteins. The RNPP family of regulatory proteins controls diverse traits, including sporulation, competence, toxin production and conjugation, in response to the direct binding of small quorum peptides to the TPR domains (reviewed in: Rocha-Estrada *et al.*, 2010, Cook & Federle, 2014). The RNPP proteins are characterized by the tetratricopeptide repeat (TPR) domains found in the C-terminal portion of these proteins. Multiple TPR domains of the RNPP proteins are arrayed in tandem, and form stacked alpha-helical surfaces that facilitate

the binding of small quorum sensing peptides (Declerck *et al.*, 2007, Diaz *et al.*, 2012). The N-terminal effector domains of RNPP proteins function as phosphatases and/or transcriptional regulators. Peptide binding to the protein induces a conformational change that either activates or inhibits the phosphatase activity or DNA-binding capabilities of an RNPP protein (Grenha *et al.*, 2013, Parashar *et al.*, 2013, Gallego del Sol & Marina, 2013, Zouhir *et al.*, 2013).

RstA contains several TPR domains that share similarity with the *Bacillus* Rap proteins; however, the conserved N-terminal HTH DNA-binding motif and predicted protein structure are more similar to the other RNPP members, namely *B. thuringiensis* PlcR and the *B. cereus* group NprR (Fig. 1). The secondary structure of PlcR, which is a DNA-binding transcriptional activator when bound to its cognate peptide (Slamti & Lereclus, 2002), aligns with residues 5–190 and 350–428 of RstA, which leaves an approximate 160 residues between the putative HTH DNA-binding motif and the C-terminal TPR domains (Fig. 1). RstA also aligns with much of the full-length bifunctional RNPP regulatory protein, NprR (Fig. 1). NprR is the only known RNPP protein that both directly binds DNA to regulate gene transcription and directly interacts with the phosphotransfer protein, Spo0F (Cabrera *et al.*, 2014). NprR contains a conserved HTH DNA-binding domain followed by a region that is similar to the Rap proteins and contains several conserved residues that mediate Spo0F binding (Cabrera *et al.*, 2014). The Spo0F-binding domain of NprR is composed of two TPR domains (Zouhir *et al.*, 2013) and is similar to the secondary structure predicted for RstA in this region (Fig. 1). Our data and the structural similarity between RstA and the other RNPP proteins suggest that RstA functions as a DNA-binding regulator and possesses a protein-binding domain.

Multiple attempts to demonstrate direct RstA binding to potential DNA targets, including a putative *sigD* promoter (P*flgB*) and the *rstA* promoter, through *in vitro* electrophoretic mobility shift assays were unsuccessful. The absence of RstA-DNA binding *in vitro* may be attributable to several factors: 1) RstA requires a cofactor, such as a small quorum sensing peptide, to bind DNA, as is the case for other RNPP proteins (Slamti & Lereclus, 2002, Perchat *et al.*, 2011); 2) the DNA fragments tested are not direct RstA targets or 3) RstA is not a DNA-binding protein. To test if RstA requires an additional cofactor to bind DNA with high affinity, concentrated supernatants from *C. difficile* 630Δ*erm* parent, the *opp app* mutant (Edwards *et al.*, 2014) or the *rstA* mutant strains grown on 70:30 sporulation agar were added to the binding reactions, but no binding was observed. It remains unclear whether *C. difficile* employs quorum sensing to regulate sporulation initiation. To our knowledge, there is no published evidence of quorum sensing regulation in *C. difficile* sporulation, and our previous study revealed that the Opp and App oligopeptide permeases negatively influence sporulation, likely through nutrient acquisition rather than quorum sensing (Edwards *et al.*, 2014). In addition, a recent study revealed that the absence of multiple Rap proteins in gastrointestinal isolates of *B. subtilis* leads to earlier Spo0A activation and cell density-independent sporulation (Serra *et al.*, 2014). *C. difficile* may also utilize similar regulatory mechanisms. However, it is also possible that the nutrient starvation occurring in the *opp app* mutant masks the loss of the potential RstA-dependent quorum sensing, resulting in the increased sporulation phenotype observed. It is important to note that the Agr quorum sensing system positively controls sporulation in other related non-

pathogenic and pathogenic clostridial organisms, including *C. acetobutylicum*, *C. botulinum* and *C. perfringens* (Cooksley *et al.*, 2010, Li *et al.*, 2011, Steiner *et al.*, 2012); however, the regulatory pathways have not been elucidated. The *C. difficile* genome contains one to two encoded *agr* systems (Darkoh *et al.*, 2015). The partial Agr1 system in *C. difficile* 630 has not been studied to our knowledge, and thus, its influence on sporulation is unknown. Finally, there remains the possibility that a host-derived signal triggers sporulation in an RstA-dependent manner.

Determining the genetic interactions through which RstA induces spore formation in *C. difficile* is a focus of future studies, as is determining how *rstA* expression and activity is controlled. Transcription of *rstA* in 630Δ*erm* varies less than 2-fold throughout sporulation, and overexpression of *rstA* in the parent background does not increase sporulation, suggesting that regulation of RstA activity is controlled post-transcriptionally. Although regulation of *sigD* transcription by RstA requires the putative DNA-binding region, this activity also likely involves specific peptide interactions mediated by the TPR repeat domains. As evidenced by the restoration of sporulation with a truncated RstAΔHTH allele expressed in the *rstA* background, RstA functions as a transcriptional regulator and has additional regulatory functions that likely require protein interaction. As a bifunctional protein, the regulatory activity of RstA is expected to be complex, as is the case for the related RNPP protein, NprR (Cabrera *et al.*, 2014).

RstA is highly conserved in all sequenced *C. difficile* genomes, suggesting that its function is conserved as well. RstA orthologs are also encoded in pathogenic and non-pathogenic *Clostridium* and closely related organisms, including *C. botulinum*, *C. perfringens*, *C. sordellii*, *C. acetobutylicum* and *C. butyricum*, which suggests an important role for RstA in clostridial physiology and pathogenesis. Although the regulation and function of the *C. difficile* sporulation-specific sigma factors and additional sporulation regulators differ from other clostridia (Fimlaid *et al.*, 2013), RstA may similarly regulate early sporulation events in both *C. difficile* and other clostridial organisms. These findings underscore the unique molecular mechanisms that *C. difficile*, and likely clostridia, use to promote virulence, sporulation, motility and toxin production, and have revealed an important regulatory protein that regulates these physiological processes during *C. difficile* infection.

EXPERIMENTAL PROCEDURES

Bacterial strains and growth conditions

The bacterial strains and plasmids used in this study are listed in Table 3. *Clostridium difficile* strains were routinely cultured in BHIS or TY broth or on BHIS agar plates and supplemented with 2–10 μg ml^{-1} thiamphenicol, 5 μg ml^{-1} erythromycin or 0.5–1 μg ml^{-1} nisin (Sigma-Aldrich) as needed (Smith *et al.*, 1981). Counterselection of *E. coli* after conjugation with *C. difficile* was performed using 50 μg ml^{-1} kanamycin as previously described (Purcell *et al.*, 2012). Taurocholate (0.1%, Sigma-Aldrich) and fructose (0.2%) were added to *C. difficile* cultures to induce germination of *C. difficile* spores and prevent sporulation, respectively, as indicated (Sorg & Dineen, 2009, Putnam *et al.*, 2013). *C. difficile* strains were cultured in an anaerobic chamber maintained at 37°C (Coy Laboratory Products) with an atmosphere of 10% H_2, 5% CO_2 and 85% N_2 as previously described

(Edwards *et al.*, 2013). *Escherichia coli* strains were grown at 37°C in LB (Luria & Burrous, 1957) or BHIS medium, unless otherwise stated, and supplemented with 20 μg ml^{-1} chloramphenicol and/or 100 μg ml^{-1} ampicillin as needed.

Strain and plasmid construction

Oligonucleotides used in this study are listed in Fig. S7. Details of DNA cloning and vector construction are outlined in Fig. S8. *C. difficile* strain 630 (Genbank no. NC_009089.1) was used as a template for primer design and *C. difficile* strain 630Δ*erm* was used for PCR amplification, unless otherwise specified. Isolation of plasmid DNA, PCR and cloning were performed using standard protocols. Additional genetic manipulations of *C. difficile* were performed as previously described (Bouillaut *et al.*, 2011). Null mutations in *C. difficile* were created by retargeting the group II intron from pCE240 using the intron retargeting primers listed in Fig. S7, as previously described (Karberg *et al.*, 2001, Ho & Ellermeier, 2011, Heap *et al.*, 2007). To complement the *CD3668* disruption, a control plasmid (pMC211; Edwards *et al.*, 2014) or plasmids containing the *CD3668* wild-type, histidine-tagged or HTH motif deletion gene driven by the *cprA* promoter (pMC367, pMC519 and pMC520; McBride & Sonenshein, 2011b, Purcell *et al.*, 2012, Suarez *et al.*, 2013) was transferred into *C. difficile* strains from *E. coli* by conjugation as previously described, except that 50 μg ml^{-1} kanamycin was used to counterselect against *E. coli* post-conjugation (McBride & Sonenshein, 2011a). Cloned DNA fragments were verified by sequencing (Eurofins MWG Operon).

Southern blot analysis

Genomic DNA from 630Δ*erm*, MC379, MC391 and RT1075 was isolated following a modified Bust n' Grab protocol (Harju *et al.*, 2004). Briefly, 6 ml of *C. difficile* culture was washed with TE Buffer (10 mM Tris-HCl pH 8.0, 1 mM EDTA pH 8.0) before the cells were suspended in 400 μl lysis buffer (2% Triton X-100, 1% SDS, 100 mM NaCl, 10 mM Tris-HCl, pH 8.0, 1 mM EDTA, pH 8.0). Cells were lysed as described except samples were exposed to a dry ice-ethanol bath for 2 min and boiled for 2 min twice. Lysed cells were removed by phenol:chloroform:isoamyl alcohol (25:24:1) extraction and subsequent chloroform extraction. Contaminating RNA was removed by incubation with RNase A (Ambion) for 30 min at 37°C. Genomic DNA was digested, separated and transferred and fixed onto Hybond-N+ nylon membranes (GE Healthcare) as previously described (Edwards *et al.*, 2014). Southern blot analysis was performed using a DIG High Prime labeling and detection kit (Roche) and an intron-specific probe (Saujet *et al.*, 2013).

Sporulation assays and phase contrast microscopy

C. difficile cultures were started in BHIS medium supplemented with 0.1% taurocholate and 0.2% fructose, to induce germination of *C. difficile* spores and prevent sporulation, respectively, until late-log phase. Cultures were then diluted in BHIS to an optical density at 600 nm (OD_{600}) of 0.5. These cultures (250 μl) were applied to 70:30 sporulation agar as a lawn (Putnam *et al.*, 2013). Plates were incubated at 37°C and monitored for the production of spores. At the indicated time points, cells were scraped from the plates, suspended in BHIS medium and removed from the chamber. Sample and slide preparation was performed as previously described (Edwards *et al.*, 2014). Phase contrast microscopy was performed

using a X100 Ph3 oil immersion objective on a Nikon Eclipse Ci-L microscope. At least two fields of view for each strain were acquired with a DS-Fi2 camera, and at least 1000 cells per independent experiment were enumerated to calculate the percentage of spores (the number of spores divided by the total number of spores and vegetative cells) from at least three independent experiments.

Ethanol resistance assays

C. difficile strains were grown on 70:30 sporulation agar as described above, and ethanol resistance assays were performed as previously described (Edwards *et al.*, 2014). Briefly, after 24 h growth (H_{24}), cells were scraped from the plates and suspended in 70:30 sporulation liquid medium to an OD_{600} = 1.0. Cells were immediately serially diluted in 70:30 sporulation liquid medium and plated onto BHIS + 0.1% taurocholate plates to enumerate all viable vegetative cells and spores. An 0.5 ml aliquot of culture was removed from the chamber, mixed with 0.5 ml 95% ethanol, vortexed and incubated at room temperature for 15 min. Ethanol-treated cells were serially diluted in 1X PBS, brought back into the chamber and plated onto BHIS + 0.1% taurocholate plates to enumerate spores. After 24 h of growth, CFU were enumerated, and the sporulation frequency was calculated as the number of ethanol resistant spores divided by the total number of viable cells. A *spo0A* mutant (MC310) was used as a negative control.

Fluorescence Microscopy

C. difficile strains were grown on 70:30 sporulation agar as described above. After 24 h growth (H_{24}), cells were scraped from the plates, suspended in 0.5 ml BHIS and pelleted at room temperature. The supernatant was removed, cells were suspended in 50 μl BHIS, and the membrane specific dyes FM4-64 and MitoTracker Green (Life Technologies) were added to the samples at a final concentration of 165 μM and 100 μM, respectively. Cells were incubated for 20 min in the dark at room temperature, and slides were prepared as previously described (Edwards *et al.*, 2014), using a 24x55 mm #1 coverslip. Fluorescence microscopy was performed using a X100 oil immersion objective (numerical aperture, 1.49) on a Nikon structured illumination microscope (N-SIM). At least three fields of view for each strain were used to calculate the percentage of cells entering sporulation from at least three independent biological replicates. The percentage of sporulating cells was defined as the number of cells possessing polar septa, partially/completely engulfed forespores or fully formed spores (stage II and beyond) divided by the total number of cells.

RNA isolation and quantitative reverse transcription PCR analysis (qRT-PCR)

Samples of *C. difficile* were grown on 70:30 sporulation agar as described above, and cells were harvested from plates directly into 1.5:1.5:3 ethanol:acetone:dH_2O. RNA was purified as previously described (Dineen *et al.*, 2010, McBride & Sonenshein, 2011b, Edwards *et al.*, 2014), and cDNA synthesis was performed as previously detailed (Edwards *et al.*, 2014). Either 50 ng (samples isolated from *in vitro* cultures) or 200 ng (samples isolated from hamster cecal content) cDNA per reaction mixture was used for quantitative reverse-transcription PCR (qRT-PCR) analysis. qRT-PCR analysis was performed using SensiFAST SYBR & Fluorescein kit (Bioline) and a Roche Lightcycler 96. Control cDNA synthesis reactions containing no reverse transcriptase were included to identify genomic

contamination. Primers for qRT-PCR analysis were designed using PrimerQuest (Integrated DNA Technologies), and primer efficiencies were calculated for each primer set prior to use. qRT-PCR was performed in technical triplicate for each cDNA sample and primer pair and on cDNA isolated from a minimum of three biological replicates. Results were calculated by the comparative cycle threshold method (Schmittgen & Livak, 2008) and normalized to the *rpoC* transcript. Results are presented as the means and standard errors of the means, and a two-tailed Student's *t* test was performed to determine statistical significance.

Motility Assays

C. difficile strains were grown overnight in BHIS medium supplemented with 0.1% taurocholate and 0.2% fructose as detailed above. Cultures were diluted to an OD_{600} of 0.5 in BHIS broth, and 5 μl of culture was stabbed in the center of one-half concentration BHI plates with 0.3% agar. The diameter of cell growth was measured every 24 h for five days, and the results represent four independent experiments. Results are presented as means and standard errors of the means, and a two-tailed Student's *t* test was performed for statistical comparison of mutant outcomes to the parent strain.

Alkaline Phosphatase (AP) Assays

AP assays were performed as previously described (Edwards *et al.*, 2015) with the following modifications. Briefly, *C. difficile* strains were grown on 70:30 sporulation agar as described above, and cells were harvested from plates at H_8 and suspended directly into 1 ml dH_2O to an OD_{600} of 0.5. Cells were pelleted and stored overnight at −20°C, and the AP assay was continued as previously described, except that no chloroform was used for cell lysis (Edwards *et al.*, 2015). Technical duplicates for each sample were performed and averaged, and results are presented as means and standard error of the means of four biological replicates. The two-tailed Student's *t* test was used to compare the results of the mutant to the parent strain.

Animal Studies

Female Syrian golden hamsters (*Mesocricetus auratus*) weighing between 75–100 g were obtained from Charles River Laboratories and housed individually in sterile cages in an animal biosafety level 2 facility in the Emory University Division of Animal Resources. Hamsters were fed a standard rodent diet and offered water *ad libitum*. Seven days prior to inoculation with *C. difficile*, the hamsters were administered one dose of clindamycin (30 mg kg^{-1} of body weight) by oral gavage to enable susceptibility to *C. difficile* infection. Hamsters were inoculated with approximately 5000 spores of a single strain of *C. difficile* (630Δ*erm* or MC391) seven days after antibiotic administration. Negative control animals were administered clindamycin to induce susceptibility to disease but were not infected with *C. difficile*. Hamsters were weighed at least daily and monitored for signs of disease (weight loss, lethargy, diarrhea and wet tail), and fecal samples were collected daily for enumeration of total *C. difficile* CFU. Hamsters were considered moribund if they lost 15% or more of their highest weight or if they presented with disease symptoms of lethargy, diarrhea and wet tail. To prevent suffering, animals meeting either criterion were euthanized by CO_2 asphyxiation and subsequent thoracotomy. At the time of death, animals were necropsied, and cecal contents were obtained for enumeration of total *C. difficile* CFU as well as stored

in 1:1 ethanol-acetone solution at −80°C for RNA isolation and subsequent qRT-PCR analysis. Two independent experiments were performed in cohorts of six animals per *C. difficile* strain. For enumeration of *C. difficile* CFU, fecal samples were weighed, and fecal and cecal samples were suspended in 1X PBS, heated to 55°C for 20 min to eliminate significant background growth of other organisms, and plated onto the *C. difficile* selective agar, taurocholate cycloserine cefoxitin fructose agar (TCCFA; George *et al.*, 1979, Wilson *et al.*, 1982). *C. difficile* colony forming units, which derived from vegetative cells and germinated spores, were enumerated after 48 h. This standard preparation of fecal samples does not significantly reduce vegetative cells numbers, and this method does not distinguish vegetative cells from spores (data not shown). Therefore, our results represent total *C. difficile* cells recovered from fecal and cecal contents. Differences in *C. difficile* CFU recovered from fecal and cecal content samples were determined by a two-tailed Student's *t* test (Excel; Microsoft), and differences in hamster survival between those infected with *C. difficile* 630Δ*erm* or MC391 were analyzed using the log rank test (GraphPad Prism 6).

Western blot analysis

Strains were grown in TY medium overnight and then diluted into fresh TY medium. After incubation for 24 h at 37°C, bacterial cells were collected by centrifugation and suspended in SDS-PAGE loading buffer (62.5 mM Tris-HCl, pH 6.8, 25% glycerol, 2% SDS, 0.01% Bromophenol Blue, 5% 2-mercaptoethanol). The samples were separated by electrophoresis on pre-cast TGX 4–15% gradient gels (BioRad), and then transferred to nitrocellulose membranes. TcdA was detected using mouse anti-TcdA antibodies (Novus Biologicals). RNA polymerase β-subunit served as a loading control and was detected using mouse anti-RNAP antibodies (Abcam). Goat anti-mouse IgG conjugated with IR800 dye was used as the secondary antibody. The blots were imaged and densitometry analyses were performed using an Odyssey imaging system (LI-COR). The intensities of the bands corresponding to TcdA were normalized to those of the RNAP band. To calculate fold changes, TcdA protein levels of each mutant were normalized to 630Δ*erm* TcdA protein levels. The data presented are the mean values and standard error of the mean of the fold changes relative to the parent strain.

Supplementary Material

Refer to Web version on PubMed Central for supplementary material.

Acknowledgments

We give special thanks to Dr. Charles Moran and members of the McBride lab for helpful suggestions and discussions during the course of this work and to Emily Weinert for advice on protein expression. This research was supported by the U.S. National Institutes of Health through research grants DK087763, DK101870, AI109526 and AI116933 to S.M.M and AI107029 to R.T.

References

Antunes A, Camiade E, Monot M, Courtois E, Barbut F, Sernova NV, Rodionov DA, Martin-Verstraete I, Dupuy B. Global transcriptional control by glucose and carbon regulator CcpA in Clostridium difficile. Nucleic acids research. 2012; 40:10701–10718. [PubMed: 22989714]

Antunes A, Martin-Verstraete I, Dupuy B. CcpA-mediated repression of Clostridium difficile toxin gene expression. Molecular microbiology. 2011; 79:882–899. [PubMed: 21299645]

Best EL, Freeman J, Wilcox MH. Models for the study of Clostridium difficile infection. Gut microbes. 2012; 3:145–167. [PubMed: 22555466]

Bongiorni C, Ishikawa S, Stephenson S, Ogasawara N, Perego M. Synergistic regulation of competence development in Bacillus subtilis by two Rap-Phr systems. Journal of bacteriology. 2005; 187:4353–4361. [PubMed: 15968044]

Bordeleau E, Purcell EB, Lafontaine DA, Fortier LC, Tamayo R, Burrus V. Cyclic di-GMP riboswitch-regulated type IV pili contribute to aggregation of Clostridium difficile. Journal of bacteriology. 2015; 197:819–832. [PubMed: 25512308]

Bouillaut L, McBride SM, Sorg JA. Genetic manipulation of Clostridium difficile. Current protocols in microbiology Chapter. 2011; 9(Unit 9A):2.

Cabrera R, Rocha J, Flores V, Vazquez-Moreno L, Guarneros G, Olmedo G, Rodriguez-Romero A, de la Torre M. Regulation of sporulation initiation by NprR and its signaling peptide NprRB: molecular recognition and conformational changes. Applied microbiology and biotechnology. 2014; 98:9399–9412. [PubMed: 25256619]

Chang JC, LaSarre B, Jimenez JC, Aggarwal C, Federle MJ. Two group A streptococcal peptide pheromones act through opposing Rgg regulators to control biofilm development. PLoS pathogens. 2011; 7:e1002190. [PubMed: 21829369]

Chang TW, Bartlett JG, Gorbach SL, Onderdonk AB. Clindamycin-induced enterocolitis in hamsters as a model of pseudomembranous colitis in patients. Infection and immunity. 1978; 20:526–529. [PubMed: 669810]

Cook LC, Federle MJ. Peptide pheromone signaling in Streptococcus and Enterococcus. FEMS microbiology reviews. 2014; 38:473–492. [PubMed: 24118108]

Cooksley CM I, Davis J, Winzer K, Chan WC, Peck MW, Minton NP. Regulation of neurotoxin production and sporulation by a Putative agrBD signaling system in proteolytic Clostridium botulinum. Applied and environmental microbiology. 2010; 76:4448–4460. [PubMed: 20453132]

Core L, Perego M. TPR-mediated interaction of RapC with ComA inhibits response regulator-DNA binding for competence development in Bacillus subtilis. Molecular microbiology. 2003; 49:1509–1522. [PubMed: 12950917]

Darkoh C, DuPont HL, Norris SJ, Kaplan HB. Toxin synthesis by Clostridium difficile is regulated through quorum signaling. mBio. 2015; 6:e02569. [PubMed: 25714717]

Deakin LJ, Clare S, Fagan RP, Dawson LF, Pickard DJ, West MR, Wren BW, Fairweather NF, Dougan G, Lawley TD. The Clostridium difficile spo0A gene is a persistence and transmission factor. Infection and immunity. 2012; 80:2704–2711. [PubMed: 22615253]

Declerck N, Bouillaut L, Chaix D, Rugani N, Slamti L, Hoh F, Lereclus D, Arold ST. Structure of PlcR: Insights into virulence regulation and evolution of quorum sensing in Gram-positive bacteria. Proceedings of the National Academy of Sciences of the United States of America. 2007; 104:18490–18495. [PubMed: 17998541]

Diaz AR, Core LJ, Jiang M, Morelli M, Chiang CH, Szurmant H, Perego M. Bacillus subtilis RapA phosphatase domain interaction with its substrate, phosphorylated Spo0F, and its inhibitor, the PhrA peptide. Journal of bacteriology. 2012; 194:1378–1388. [PubMed: 22267516]

Dineen SS, McBride SM, Sonenshein AL. Integration of metabolism and virulence by Clostridium difficile CodY. Journal of bacteriology. 2010; 192:5350–5362. [PubMed: 20709897]

Dineen SS, Villapakkam AC, Nordman JT, Sonenshein AL. Repression of Clostridium difficile toxin gene expression by CodY. Molecular microbiology. 2007; 66:206–219. [PubMed: 17725558]

Douce G, Goulding D. Refinement of the hamster model of Clostridium difficile disease. Methods Mol Biol. 2010; 646:215–227. [PubMed: 20597012]

Edwards AN, McBride SM. Initiation of sporulation in Clostridium difficile: a twist on the classic model. FEMS microbiology letters. 2014

Edwards AN, Nawrocki KL, McBride SM. Conserved Oligopeptide Permeases Modulate Sporulation Initiation in Clostridium difficile. Infection and immunity. 2014; 82:4276–4291. [PubMed: 25069979]

Edwards AN, Pascual RA, Childress KO, Nawrocki KL, Woods EC, McBride SM. An alkaline phosphatase reporter for use in Clostridium difficile. Anaerobe. 2015

Edwards AN, Suarez JM, McBride SM. Culturing and Maintaining Clostridium difficile in an Anaerobic Environment. Journal of visualized experiments: JoVE. 2013

El Meouche I, Peltier J, Monot M, Soutourina O, Pestel-Caron M, Dupuy B, Pons JL. Characterization of the SigD regulon of C. difficile and its positive control of toxin production through the regulation of tcdR. PloS one. 2013; 8:e83748. [PubMed: 24358307]

Errington J. Regulation of endospore formation in Bacillus subtilis. Nature reviews Microbiology. 2003; 1:117–126. [PubMed: 15035041]

Fimlaid KA, Bond JP, Schutz KC, Putnam EE, Leung JM, Lawley TD, Shen A. Global Analysis of the Sporulation Pathway of Clostridium difficile. PLoS genetics. 2013; 9:e1003660. [PubMed: 23950727]

Gallego del Sol F, Marina A. Structural basis of Rap phosphatase inhibition by Phr peptides. PLoS biology. 2013; 11:e1001511. [PubMed: 23526880]

George WL V, Sutter L, Citron D, Finegold SM. Selective and differential medium for isolation of Clostridium difficile. Journal of clinical microbiology. 1979; 9:214–219. [PubMed: 429542]

Gominet M, Slamti L, Gilois N, Rose M, Lereclus D. Oligopeptide permease is required for expression of the Bacillus thuringiensis plcR regulon and for virulence. Molecular microbiology. 2001; 40:963–975. [PubMed: 11401703]

Grenha R, Slamti L, Nicaise M, Refes Y, Lereclus D, Nessler S. Structural basis for the activation mechanism of the PlcR virulence regulator by the quorum-sensing signal peptide PapR. Proceedings of the National Academy of Sciences of the United States of America. 2013; 110:1047–1052. [PubMed: 23277548]

Harju S, Fedosyuk H, Peterson KR. Rapid isolation of yeast genomic DNA: Bust n' Grab. BMC biotechnology. 2004; 4:8. [PubMed: 15102338]

Heap JT, Pennington OJ, Cartman ST, Carter GP, Minton NP. The ClosTron: a universal gene knock-out system for the genus Clostridium. Journal of microbiological methods. 2007; 70:452–464. [PubMed: 17658189]

Ho TD, Ellermeier CD. PrsW is required for colonization, resistance to antimicrobial peptides, and expression of extracytoplasmic function sigma factors in Clostridium difficile. Infection and immunity. 2011; 79:3229–3238. [PubMed: 21628514]

Hussain HA, Roberts AP, Mullany P. Generation of an erythromycin-sensitive derivative of Clostridium difficile strain 630 (630Δerm) and demonstration that the conjugative transposon Tn916ΔE enters the genome of this strain at multiple sites. Journal of medical microbiology. 2005; 54:137–141. [PubMed: 15673506]

Jiang M, Grau R, Perego M. Differential processing of propeptide inhibitors of Rap phosphatases in Bacillus subtilis. Journal of bacteriology. 2000; 182:303–310. [PubMed: 10629174]

Karberg M, Guo H, Zhong J, Coon R, Perutka J, Lambowitz AM. Group II introns as controllable gene targeting vectors for genetic manipulation of bacteria. Nature biotechnology. 2001; 19:1162–1167.

Karlsson S, Burman LG, Akerlund T. Induction of toxins in Clostridium difficile is associated with dramatic changes of its metabolism. Microbiology. 2008; 154:3430–3436. [PubMed: 18957596]

Karpenahalli MR, Lupas AN, Soding J. TPRpred: a tool for prediction of TPR-, PPR- and SEL1-like repeats from protein sequences. BMC bioinformatics. 2007; 8:2. [PubMed: 17199898]

Kelley LA, Mezulis S, Yates CM, Wass MN, Sternberg MJ. The Phyre2 web portal for protein modeling, prediction and analysis. Nature protocols. 2015; 10:845–858. [PubMed: 25950237]

Koide A, Hoch JA. Identification of a second oligopeptide transport system in Bacillus subtilis and determination of its role in sporulation. Molecular microbiology. 1994; 13:417–426. [PubMed: 7997159]

Kuehne SA, Cartman ST, Heap JT, Kelly ML, Cockayne A, Minton NP. The role of toxin A and toxin B in Clostridium difficile infection. Nature. 2010; 467:711–713. [PubMed: 20844489]

Lazazzera BA I, Kurtser G, McQuade RS, Grossman AD. An autoregulatory circuit affecting peptide signaling in Bacillus subtilis. Journal of bacteriology. 1999; 181:5193–5200. [PubMed: 10464187]

Lazazzera BA, Solomon JM, Grossman AD. An exported peptide functions intracellularly to contribute to cell density signaling in B. subtilis. Cell. 1997; 89:917–925. [PubMed: 9200610]

Leonard BA, Podbielski A, Hedberg PJ, Dunny GM. Enterococcus faecalis pheromone binding protein, PrgZ, recruits a chromosomal oligopeptide permease system to import sex pheromone cCF10 for induction of conjugation. Proceedings of the National Academy of Sciences of the United States of America. 1996; 93:260–264. [PubMed: 8552617]

Lereclus D, Agaisse H, Gominet M, Salamitou S, Sanchis V. Identification of a Bacillus thuringiensis gene that positively regulates transcription of the phosphatidylinositol-specific phospholipase C gene at the onset of the stationary phase. Journal of bacteriology. 1996; 178:2749–2756. [PubMed: 8631661]

Li J, Chen J, Vidal JE, McClane BA. The Agr-like quorum-sensing system regulates sporulation and production of enterotoxin and beta2 toxin by Clostridium perfringens type A non-food-borne human gastrointestinal disease strain F5603. Infection and immunity. 2011; 79:2451–2459. [PubMed: 21464088]

Losick R, Stragier P. Crisscross regulation of cell-type-specific gene expression during development in B. subtilis. Nature. 1992; 355:601–604. [PubMed: 1538747]

Luria SE, Burrous JW. Hybridization between *Escherichia coli* and *Shigella*. J Bacteriol. 1957; 74:461–476. [PubMed: 13475269]

Mackin KE, Carter GP, Howarth P, Rood JI, Lyras D. Spo0A differentially regulates toxin production in evolutionarily diverse strains of Clostridium difficile. PloS one. 2013; 8:e79666. [PubMed: 24236153]

Manganelli R, Provvedi R, Berneri C, Oggioni MR, Pozzi G. Insertion vectors for construction of recombinant conjugative transposons in *Bacillus subtilis* and *Enterococcus faecalis*. FEMS Microbiol Lett. 1998; 168:259–268. [PubMed: 9835037]

Mani N, Dupuy B. Regulation of toxin synthesis in Clostridium difficile by an alternative RNA polymerase sigma factor. Proceedings of the National Academy of Sciences of the United States of America. 2001; 98:5844–5849. [PubMed: 11320220]

Mashburn-Warren L, Morrison DA, Federle MJ. A novel double-tryptophan peptide pheromone controls competence in Streptococcus spp. via an Rgg regulator. Molecular microbiology. 2010; 78:589–606. [PubMed: 20969646]

McBride SM. More Than One Way to Make a Spore. Microbe. 2014; 9:153–157.

McBride SM, Sonenshein AL. The dlt operon confers resistance to cationic antimicrobial peptides in Clostridium difficile. Microbiology. 2011a; 157:1457–1465. [PubMed: 21330441]

McBride SM, Sonenshein AL. Identification of a genetic locus responsible for antimicrobial peptide resistance in Clostridium difficile. Infection and immunity. 2011b; 79:167–176. [PubMed: 20974818]

McKee RW, Mangalea MR, Purcell EB, Borchardt EK, Tamayo R. The second messenger cyclic Di-GMP regulates Clostridium difficile toxin production by controlling expression of sigD. Journal of bacteriology. 2013; 195:5174–5185. [PubMed: 24039264]

Mueller JP, Sonenshein AL. Role of the Bacillus subtilis gsiA gene in regulation of early sporulation gene expression. Journal of bacteriology. 1992; 174:4374–4383. [PubMed: 1624431]

Parashar V, Aggarwal C, Federle MJ, Neiditch MB. Rgg protein structure-function and inhibition by cyclic peptide compounds. Proceedings of the National Academy of Sciences of the United States of America. 2015; 112:5177–5182. [PubMed: 25847993]

Parashar V, Jeffrey PD, Neiditch MB. Conformational change-induced repeat domain expansion regulates Rap phosphatase quorum-sensing signal receptors. PLoS biology. 2013; 11:e1001512. [PubMed: 23526881]

Parashar V, Mirouze N, Dubnau DA, Neiditch MB. Structural basis of response regulator dephosphorylation by Rap phosphatases. PLoS biology. 2011; 9:e1000589. [PubMed: 21346797]

Paredes-Sabja D, Shen A, Sorg JA. Clostridium difficile spore biology: sporulation, germination, and spore structural proteins. Trends in microbiology. 2014; 22:406–416. [PubMed: 24814671]

Paredes CJ, Alsaker KV, Papoutsakis ET. A comparative genomic view of clostridial sporulation and physiology. Nature reviews Microbiology. 2005; 3:969–978. [PubMed: 16261177]

Perchat S, Dubois T, Zouhir S, Gominet M, Poncet S, Lemy C, Aumont-Nicaise M, Deutscher J, Gohar M, Nessler S, Lereclus D. A cell-cell communication system regulates protease production

during sporulation in bacteria of the Bacillus cereus group. Molecular microbiology. 2011; 82:619–633. [PubMed: 21958299]

Perego M. A peptide export-import control circuit modulating bacterial development regulates protein phosphatases of the phosphorelay. Proceedings of the National Academy of Sciences of the United States of America. 1997; 94:8612–8617. [PubMed: 9238025]

Perego M, Hanstein C, Welsh KM, Djavakhishvili T, Glaser P, Hoch JA. Multiple protein-aspartate phosphatases provide a mechanism for the integration of diverse signals in the control of development in B. subtilis. Cell. 1994; 79:1047–1055. [PubMed: 8001132]

Perego M, Higgins CF, Pearce SR, Gallagher MP, Hoch JA. The oligopeptide transport system of Bacillus subtilis plays a role in the initiation of sporulation. Molecular microbiology. 1991; 5:173–185. [PubMed: 1901616]

Perego M, Hoch JA. Cell-cell communication regulates the effects of protein aspartate phosphatases on the phosphorelay controlling development in Bacillus subtilis. Proceedings of the National Academy of Sciences of the United States of America. 1996; 93:1549–1553. [PubMed: 8643670]

Pereira FC, Saujet L, Tome AR, Serrano M, Monot M, Couture-Tosi E, Martin-Verstraete I, Dupuy B, Henriques AO. The Spore Differentiation Pathway in the Enteric Pathogen Clostridium difficile. PLoS genetics. 2013; 9:e1003782. [PubMed: 24098139]

Pettit LJ, Browne HP, Yu L, Smits WK, Fagan RP, Barquist L, Martin MJ, Goulding D, Duncan SH, Flint HJ, Dougan G, Choudhary JS, Lawley TD. Functional genomics reveals that Clostridium difficile Spo0A coordinates sporulation, virulence and metabolism. BMC genomics. 2014; 15:160. [PubMed: 24568651]

Purcell EB, McKee RW, McBride SM, Waters CM, Tamayo R. Cyclic diguanylate inversely regulates motility and aggregation in Clostridium difficile. Journal of bacteriology. 2012; 194:3307–3316. [PubMed: 22522894]

Putnam EE, Nock AM, Lawley TD, Shen A. SpoIVA and SipL are Clostridium difficile spore morphogenetic proteins. Journal of bacteriology. 2013; 195:1214–1225. [PubMed: 23292781]

Rocha-Estrada J, Aceves-Diez AE, Guarneros G, de la Torre M. The RNPP family of quorum-sensing proteins in Gram-positive bacteria. Applied microbiology and biotechnology. 2010; 87:913–923. [PubMed: 20502894]

Rosenbusch KE, Bakker D, Kuijper EJ, Smits WK. C. difficile 630Deltaerm Spo0A regulates sporulation, but does not contribute to toxin production, by direct high-affinity binding to target DNA. PloS one. 2012; 7:e48608. [PubMed: 23119071]

Rudner DZ, LeDeaux JR, Ireton K, Grossman AD. The spo0K locus of Bacillus subtilis is homologous to the oligopeptide permease locus and is required for sporulation and competence. Journal of bacteriology. 1991; 173:1388–1398. [PubMed: 1899858]

Saujet L, Monot M, Dupuy B, Soutourina O, Martin-Verstraete I. The key sigma factor of transition phase, SigH, controls sporulation, metabolism, and virulence factor expression in Clostridium difficile. Journal of bacteriology. 2011; 193:3186–3196. [PubMed: 21572003]

Saujet L, Pereira FC, Serrano M, Soutourina O, Monot M, Shelyakin PV, Gelfand MS, Dupuy B, Henriques AO, Martin-Verstraete I. Genome-Wide Analysis of Cell Type-Specific Gene Transcription during Spore Formation in Clostridium difficile. PLoS genetics. 2013; 9:e1003756. [PubMed: 24098137]

Schmittgen TD, Livak KJ. Analyzing real-time PCR data by the comparative C(T) method. Nature protocols. 2008; 3:1101–1108. [PubMed: 18546601]

Sebaihia M, Wren BW, Mullany P, Fairweather NF, Minton N, Stabler R, Thomson NR, Roberts AP, Cerdeno-Tarraga AM, Wang H, Holden MT, Wright A, Churcher C, Quail MA, Baker S, Bason N, Brooks K, Chillingworth T, Cronin A, Davis P, Dowd L, Fraser A, Feltwell T, Hance Z, Holroyd S, Jagels K, Moule S, Mungall K, Price C, Rabbinowitsch E, Sharp S, Simmonds M, Stevens K, Unwin L, Whithead S, Dupuy B, Dougan G, Barrell B, Parkhill J. The multidrug-resistant human pathogen Clostridium difficile has a highly mobile, mosaic genome. Nature genetics. 2006; 38:779–786. [PubMed: 16804543]

Serra CR, Earl AM, Barbosa TM, Kolter R, Henriques AO. Sporulation during growth in a gut isolate of Bacillus subtilis. Journal of bacteriology. 2014; 196:4184–4196. [PubMed: 25225273]

Slamti L, Lereclus D. A cell-cell signaling peptide activates the PlcR virulence regulon in bacteria of the Bacillus cereus group. The EMBO journal. 2002; 21:4550–4559. [PubMed: 12198157]

Smith CJ, Markowitz SM, Macrina FL. Transferable tetracycline resistance in Clostridium difficile. Antimicrobial agents and chemotherapy. 1981; 19:997–1003. [PubMed: 7271279]

Solomon JM, Lazazzera BA, Grossman AD. Purification and characterization of an extracellular peptide factor that affects two different developmental pathways in Bacillus subtilis. Genes & development. 1996; 10:2014–2024. [PubMed: 8769645]

Sorg JA, Dineen SS. Laboratory maintenance of Clostridium difficile. Current protocols in microbiology Chapter. 2009; 9(Unit9A):1.

Steiner E, Scott J, Minton NP, Winzer K. An agr quorum sensing system that regulates granulose formation and sporulation in Clostridium acetobutylicum. Applied and environmental microbiology. 2012; 78:1113–1122. [PubMed: 22179241]

Suarez JM, Edwards AN, McBride SM. The Clostridium difficile cpr Locus is Regulated by a Non-contiguous Two-component System in Response to Type A and B Lantibiotics. Journal of bacteriology. 2013

Thomas CM, Smith CA. Incompatibility group P plasmids: genetics, evolution, and use in genetic manipulation. Annu Rev Microbiol. 1987; 41:77–101. [PubMed: 3318684]

Underwood S, Guan S, Vijayasubhash V, Baines SD, Graham L, Lewis RJ, Wilcox MH, Stephenson K. Characterization of the sporulation initiation pathway of Clostridium difficile and its role in toxin production. Journal of bacteriology. 2009; 191:7296–7305. [PubMed: 19783633]

Wilson KH, Kennedy MJ, Fekety FR. Use of sodium taurocholate to enhance spore recovery on a medium selective for Clostridium difficile. Journal of clinical microbiology. 1982; 15:443–446. [PubMed: 7076817]

Wust J, Hardegger U. Transferable resistance to clindamycin, erythromycin, and tetracycline in *Clostridium difficile*. Antimicrob Agents Chemother. 1983; 23:784–786. [PubMed: 6870225]

Zouhir S, Perchat S, Nicaise M, Perez J, Guimaraes B, Lereclus D, Nessler S. Peptide-binding dependent conformational changes regulate the transcriptional activity of the quorum-sensor NprR. Nucleic acids research. 2013; 41:7920–7933. [PubMed: 23793817]

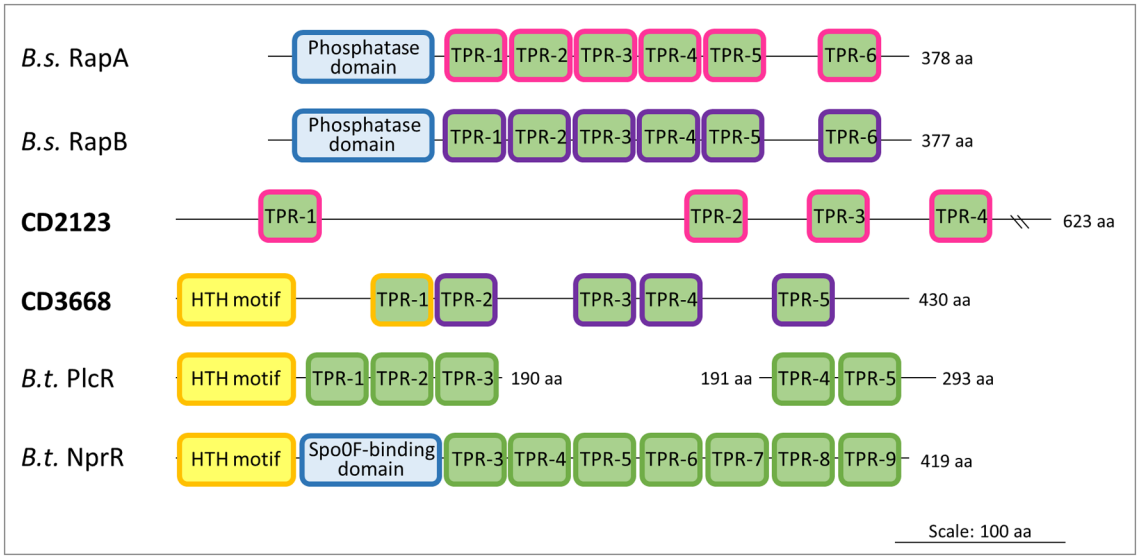

Figure 1. Identification of putative Rap orthologs in *C. difficile*

Comparison of *C. difficile* 630 (Genbank no. AM180355) CD2123 and CD3668 to the RapA and RapB proteins of *B. subtilis* 168 (AL009126), and of CD3668 to the PlcR (AVF21202.1) and NprR (ABK83928) proteins of *B. thuringiensis*. Similarity to tetratricopeptide repeat (TPR) domains were determined through BLAST and TPRpred (Karpenahalli *et al.*, 2007) analyses. TPR domain similarity is represented by outlines in pink (*B.s.* RapA), purple (*B.s.* RapB) and orange (*B.s.* RapE), while the TPR motifs outlined in green correlate to those found in *B. thuringiensis*. The Spo0F-binding domain of *B. thuringiensis* NprR is composed of TPR domains 1 and 2. Additional conserved protein domains are included.

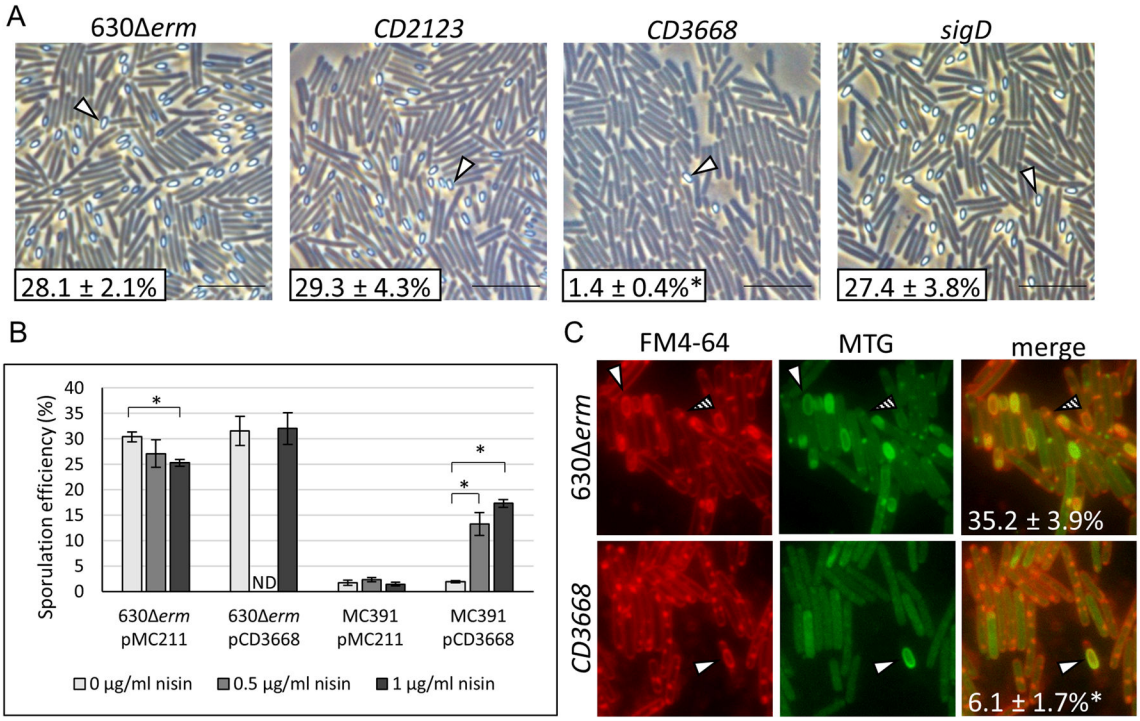

Figure 2. Sporulation is unaffected in a *CD2123* mutant and significantly decreased in a *CD3668* mutant

(A) Representative phase contrast micrographs of 630Δ*erm* and the *CD2123* (MC379), *CD3668* (MC391) and *sigD* (RT1075) mutants grown on 70:30 sporulation agar at H_{24}. Open arrowheads indicate phase bright spores. Scale bars represent 10 µm. (B) Sporulation frequency of 630Δ*erm* pMC211 (MC282, vector control), 630Δ*erm* pP*cprA::CD3668* (MC478), *CD3668* pMC211 (MC505, vector control) and *CD3668* pP*cprA-CD3668* (MC480) grown on 70:30 sporulation agar supplemented with 2 µg ml^{-1} thiamphenicol and in the absence or presence of 0.5 µg ml^{-1} and 1 µg ml^{-1} nisin. Sporulation frequency is calculated from phase contrast micrographs obtained at H_{24}. ND = not determined. (C) Fluorescence microscopy of 630Δ*erm* and the *CD3668* mutant using the membrane-specific dyes FM4-64 and Mitotracker Green (MTG). Open arrowheads point to partially or completely engulfed prespores and spores, while hatched arrowheads indicate polar septa. For phase contrast and fluorescence microscopy, samples were removed at the indicated times and prepared for microscopy as described in the Experimental Procedures. The percentage of total cells at Stage II+ are shown. The means and standard error of the means of at least four biological replicates are shown (*, $P \leq 0.05$ by a two-tailed Student's *t* test).

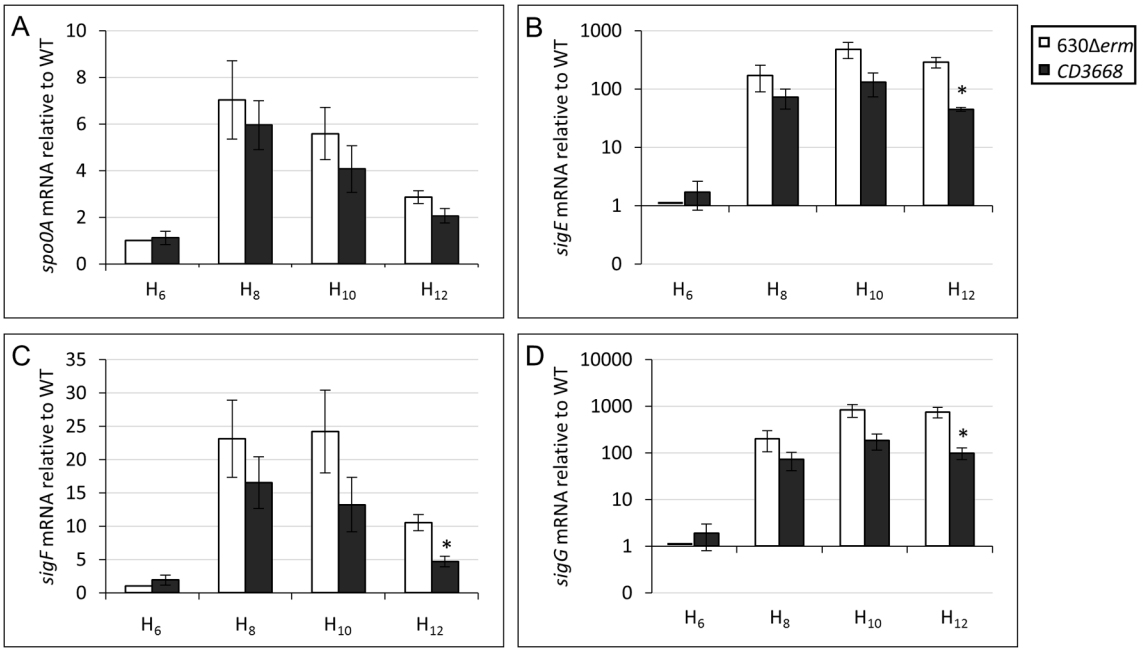

Figure 3. Sporulation-specific gene expression is decreased in a *CD3668* mutant

qRT-PCR analysis of (A) *spo0A* and the sporulation-specific sigma factors, (B) *sigE*, (C) *sigF* and (D) *sigG* expression in 630Δ*erm* and *CD3668* (MC391) grown on 70:30 sporulation agar at H_6, H_8, H_{10} and H_{12}. The means and standard error of the means of four biological replicates are shown (*, $P \leq 0.05$ by a two-tailed Student's *t* test).

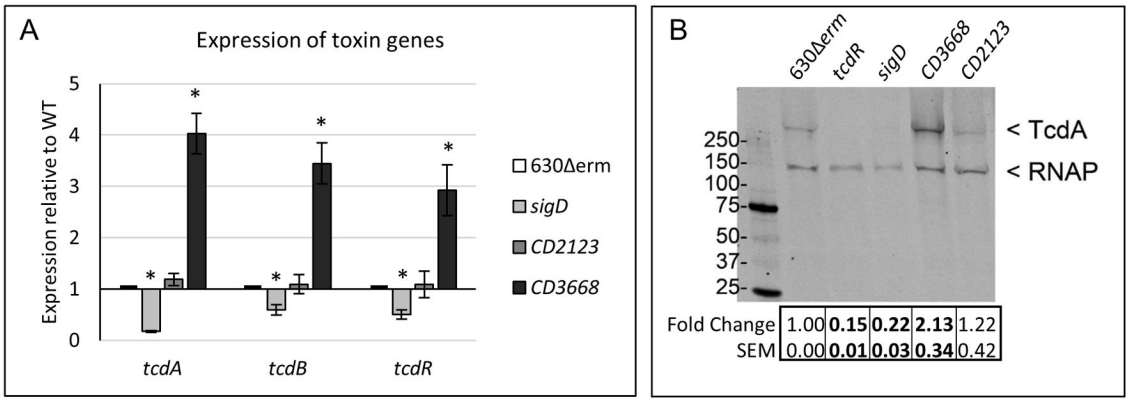

Figure 4. Toxin gene expression and TcdA protein levels are increased in a *CD3668* mutant

(A) qRT-PCR analysis of *tcdA*, *tcdB* and *tcdR* in 630Δ*erm*, *sigD* (RT1075), *CD2123* (MC379) and *CD3668* (MC391) grown on 70:30 sporulation agar at H_{12}. The means and standard error of the means of four biological replicates are shown (*, $P \leq 0.05$ by a two-tailed Student's *t* test). (B) Western blot analysis of TcdA and RNAP (RpoB′) in 630Δ*erm*, *tcdR* (RT854), *sigD* (RT1075), *CD3668* (MC391) and *CD2123* (MC379) grown in TY medium at 24 h. The means and standard error of the means of three biological replicates are shown, and bold text indicates $P \leq 0.05$ by a two-tailed Student's *t* test.

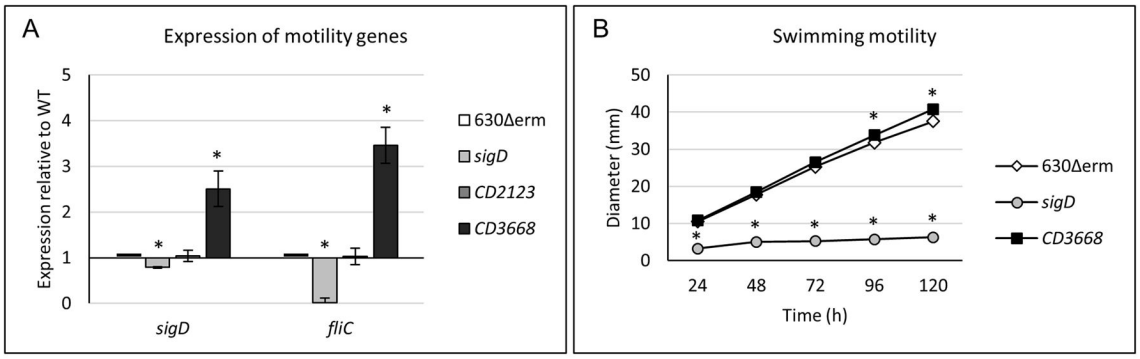

Figure 5. CD3668 represses *sigD* gene expression and motility

(A) qRT-PCR analysis of *sigD* and *fliC* in 630Δ*erm*, *sigD* (RT1075), *CD2123* (MC379) and *CD3668* (MC391) grown on 70:30 sporulation agar at H_{12}. The means and standard error of the means of four biological replicates are shown (*, $P \leq 0.05$ by a two-tailed Student's *t* test). (B) Swimming of 630Δ*erm*, *sigD* (RT1075) and *CD3668* (MC391) in one-half concentration BHI with 0.3% agar. The swim diameters (mm) were measured every 24 h for a total of 120 h. The means and standard error of the means of four biological replicates are shown (*, $P \leq 0.05$ by a two-tailed Student's *t* test). Where error bars are not visible, they are obscured by the symbols.

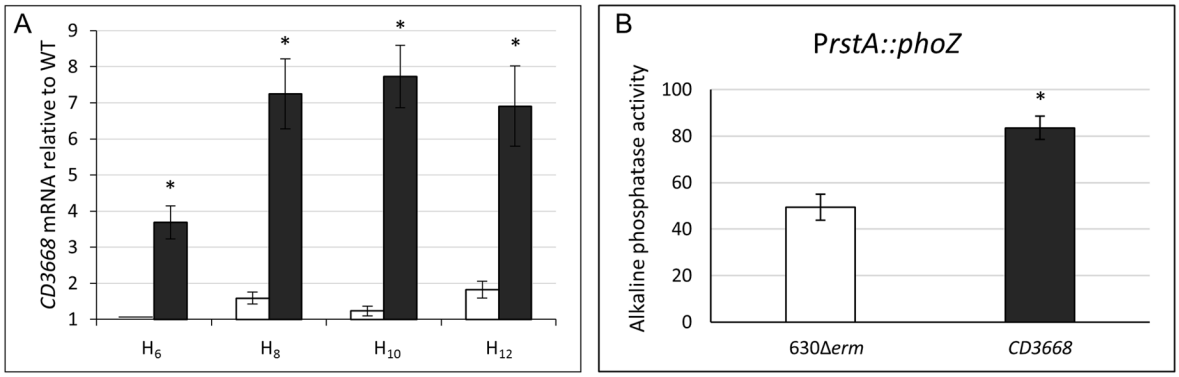

Figure 6. Expression of *rstA* is increased in the *rstA* mutant

(A) qRT-PCR analysis of *CD3668* in 630Δ*erm* and *CD3668* (MC391) grown on 70:30 sporulation agar at H_6, H_8, H_{10} and H_{12}. (B) Alkaline phosphatase (AP) activity of the P*rstA::phoZ* reporter fusion in 630Δ*erm* and *CD3668* (MC391) grown on 70:30 sporulation agar at H_8. The means and standard error of the means of four biological replicates are shown (*, $P \leq 0.05$ by a two-tailed Student's *t* test).

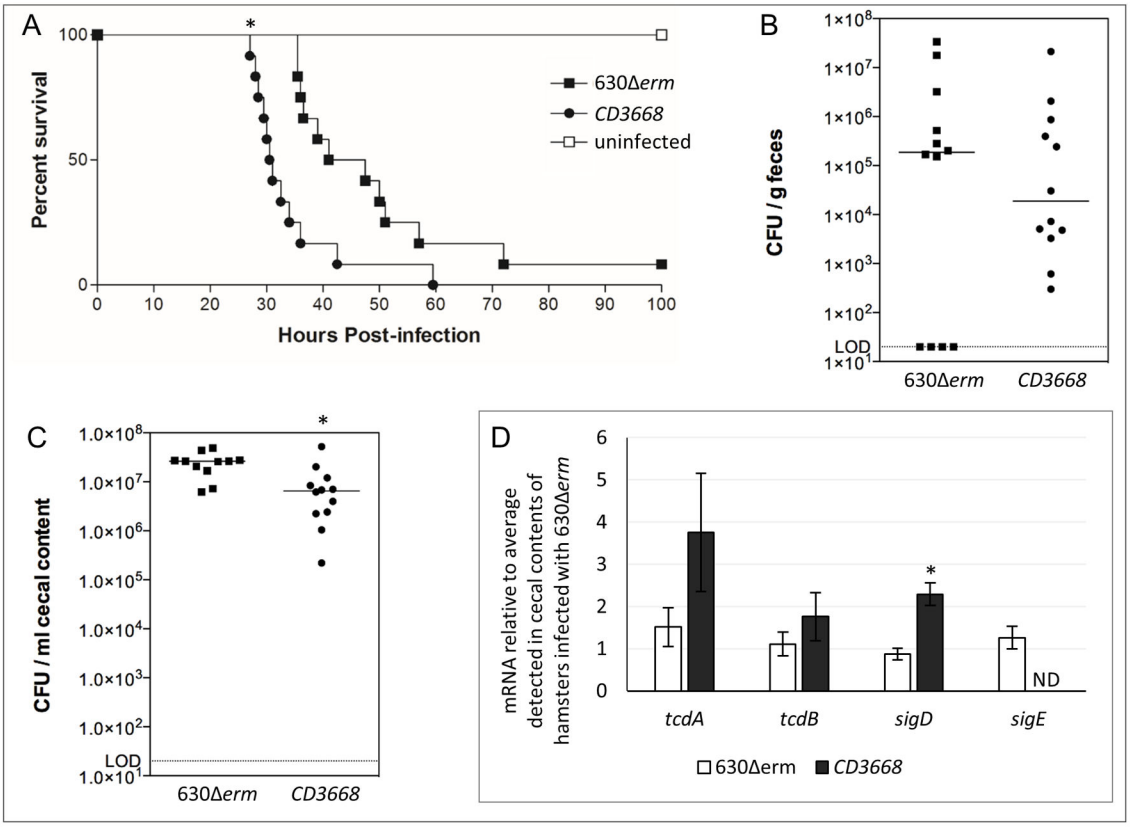

Figure 7. Disruption of *CD3668* results in increased morbidity in the hamster model of *C. difficile* infection

(A) Kaplan-Meier survival curve representing the cumulative results from two independent experiments of clindamycin-treated Syrian golden hamsters inoculated with 5000 spores of *C. difficile* 630Δ*erm* (n = 12) or MC391 (*CD3668*; n = 12). Mean times to morbidity were: 630Δ*erm*, 45.5 ± 3.5 h (n = 11); *CD3668* (MC391), 34.1 ± 2.6 h (n = 12); $P < 0.01$, log rank test. Total number of *C. difficile* colony forming units (CFU) per (B) gram of feces recovered at 24 h post infection or (C) ml of cecal content recovered at time of morbidity from the same two independent experiments described in the legend for panel A (*, $P \leq 0.05$ by a two-tailed Student's *t* test). Solid lines represent the median for each strain; dotted line denotes the limit of detection (2 x 10^1 CFU/g or CFU/ml). (D) qRT-PCR analysis of *tcdA*, *tcdB*, *sigD* and *sigE* transcript levels in cecal contents of hamsters infected with 630Δ*erm* (n = 9 for *tcdA* and *sigE* analyses; n = 10 for *tcdB* and *sigD* analyses) or MC391 (*CD3668*; n = 9 for *tcdA* analysis; n = 8 for *tcdB* and *sigD* analyses). The means and standard error of the means are shown (*, $P \leq 0.05$ by a two-tailed Student's *t* test; ND, not detected)

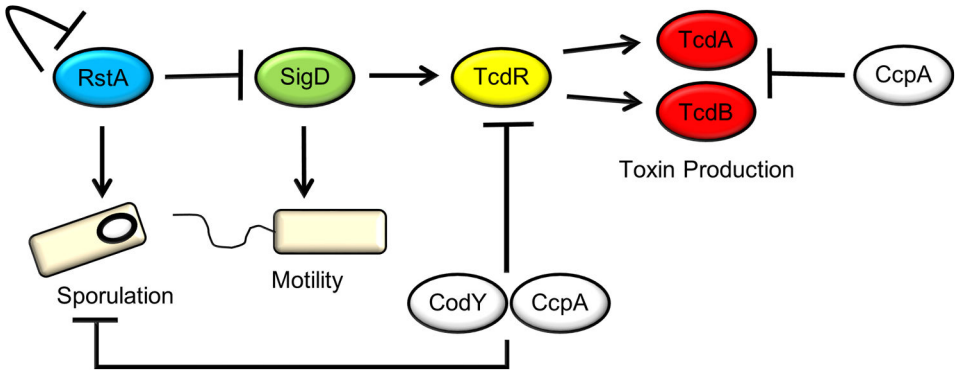

Figure 8.

Model of *C. difficile* toxin and sporulation regulation. RstA negatively impacts its own expression. RstA positively affects sporulation through an undetermined regulatory pathway. RstA negatively influences both motility and toxin production through the flagellar-specific sigma factor, SigD. In addition, CodY directly represses *tcdR* transcription (Dineen *et al.*, 2007), and CcpA directly represses *tcdR*, *tcdA* and *tcdB* gene expression (Antunes *et al.*, 2011, Antunes *et al.*, 2012). However, CodY- and CcpA-dependent toxin regulation is not influenced by RstA in the conditions tested.

Table 1

Sporulation frequency of 630Δ*erm* and the *CD3668* mutant at H_{24}

Viable cells and ethanol resistant spores (CFU ml^{-1}) represent the mean values obtained from four biological replicates grown in the conditions described in the Experimental Procedures.

Strain	Relevant Genotype	Viable cells (CFU ml^{-1})	Ethanol resistant spores (CFU ml^{-1})	Sporulation frequency	Percent Sporulation
630Δ*erm*	Parent	1.65×10^{8}	1.13×10^{7}	6.84×10^{-2}	6.84%
MC391	*CD3668::erm*	3.07×10^{8}	9.11×10^{5}	2.97×10^{-3}	0.30%

Table 2

Sporulation frequency and SigD-dependent gene expression in *C. difficile* expressing modified *rstA* derivatives.

Strain	Nis[a]	Spo %[b]	Transcript levels[c]		
			fliC	*tcdA*	*tcdB*
MC282 (630Δ*erm* pMC211[d])	−	28.2 ± 3.8%	1.0	1.0	1.0
	+	24.2 ± 3.0%	0.8 ± 0.0	1.2 ± 0.1	1.0 ± 0.1
MC505 (*rstA* pMC211[d])	−	2.1 ± 0.6%	6.6 ± 0.8	5.7 ± 1.2	3.6 ± 0.3
	+	1.4 ± 0.3%	6.1 ± 0.6	5.4 ± 0.6	3.5 ± 0.2
MC480 (*rstA* pP*cpr::rstA*)	−	2.1 ± 0.4%	6.2 ± 0.7	4.9 ± 0.6	3.1 ± 0.6
	+	**11.9 ± 3.1%**	**2.0 ± 0.6**	**1.5 ± 0.1**	**1.1 ± 0.1**
MC737 (*rstA* pP*cpr::rstA-His*)	−	1.9 ± 0.4%	3.0 ± 0.6	5.0 ± 0.8	3.3 ± 0.7
	+	**8.8 ± 2.4%**	2.0 ± 0.4	**2.1 ± 0.3**	**1.4 ± 0.2**
MC738 (*rstA* pP*cpr::rstAΔHTH-His*)	−	2.9 ± 0.7%	3.9 ± 0.6	5.2 ± 0.8	3.3 ± 0.5
	+	**5.7 ± 0.3%**	3.1 ± 0.7	3.5 ± 0.8	2.4 ± 0.2

[a] Induction with 1 μg ml^{-1} nisin.

[b] Sporulation frequency enumerated from phase contrast microscopy; bold indicates $P \leq 0.05$ by Student's *t* test compared to uninduced samples.

[c] Transcript levels were determined by qRT-PCR as described in the Experimental Procedures.

[d] pMC211 is the vector control.

Table 3

Bacterial strains and plasmids

Plasmid or Strain	Relevant genotype or features	Source, construction or reference
Strains		
E. coli		
DH5αMax	F$^-$ φ80*lac*ZΔM15 Δ(*lac*ZYA-*arg*F)	Invitrogen
Efficiency	U169 *rec*A1 *end*A1 *hsd*R17 (rk$^-$, mk$^+$) *pho*A *sup*E44 λ$^-$ *thi*$^-$1 *gyr*A96 *rel*A1	
MC101	HB101 pRK24	B. Dupuy
MC277	HB101 containing pRK24 and pMC211	(Edwards *et al.*, 2014)
MC369	HB101 containing pRK24 and pMC303	This study
MC385	HB101 containing pRK24 and pMC325	This study
MC460	HB101 containing pRK24 and pMC367	This study
MC734	HB101 containing pRK24 and pMC519	This study
MC735	HB101 containing pRK24 and pMC520	This study
MC772	HB101 containing pRK24 and pMC543	This study
C. difficile		
630	Clinical isolate	(Wust & Hardegger, 1983)
630Δ*erm*	Erm^S derivative of strain 630	N. Minton and (Hussain *et al.*, 2005)
MC282	630Δ*erm* pMC211	(Edwards *et al.*, 2014)
MC310	630Δ*erm spo0A::erm*	(Edwards *et al.*, 2014)
MC379	630Δ*erm CD2123::erm*	This study
MC391	630Δ*erm rstA::erm*	This study
MC478	630Δ*erm* pMC367	This study
MC480	630Δ*erm rstA::erm* pMC367	This study
MC505	630Δ*erm rstA::erm* pMC211	This study
MC737	630Δ*erm rstA::erm* pMC519	This study
MC738	630Δ*erm rstA::erm* pMC520	This study
MC773	630Δ*erm* pMC543 (P*rstA::phoZ*)	This study
MC774	630Δ*erm rstA::erm* pMC543 (P*rstA::phoZ*)	This study
RT854	630Δ*erm tcdR::erm*	(McKee *et al.*, 2013)
RT1075	630Δ*erm sigD::erm*	(Bordeleau *et al.*, 2015)
Plasmids		
pRK24	Tra$^+$, Mob$^+$; *bla, tet*	(Thomas & Smith, 1987)
pCR2.1	*bla, kan*	Invitrogen
pCE240	*C. difficile* TargeTron® construct based on pJIR750ai (group II intron, *ermB::*RAM, *ltrA*); *catP*	C. Ellermeier
pSMB47	Tn*916* integrational vector; CmR, ErmR	(Manganelli *et al.*, 1998)
pMC123	*E. coli-C. difficile* shuttle vector; *bla, catP*	(McBride & Sonenshein, 2011b)
pMC211	pMC123 with *cprA* promoter, *bla catP*	(Edwards *et al.*, 2014)
pMC289	pCR2.1 with group II intron targeted to *CD2123*	This study
pMC292	pCE240 with *CD2123*-targeted intron	This study
pMC303	pMC123 with *CD2123*-targeted intron, *ermB::*RAM, *ltrA; catP*	This study

Plasmid or Strain	Relevant genotype or features	Source, construction or reference
pMC320	pCR2.1 with group II intron targeted to *CD3668* (*rsdA*)	This study
pMC323	pCE240 with *CD3668*-targeted intron	This study
pMC325	pMC123 with *CD3668*-targeted intron, *ermB::*RAM, *ltrA; catP*	This study
pMC358	pMC123 *phoZ*	(Edwards *et al.*, 2015)
pMC367	pMC211 *CD3668*	This study
pMC519	pMC211 *CD3668-HIS6x*	This study
pMC520	pMC211 *CD3668ΔHTH- HIS6x*	This study
pMC543	pMC358 P*rstA::phoZ*	This study